This is a repository copy of *Generalised Modelling, Simulation and Control Design for Manipulators with Flexible Links and Flexible/Rigid Joints*.

White Rose Research Online URL for this paper:
http://eprints.whiterose.ac.uk/83057/

Monograph:
Subudhi , B. and Morris, A.S. (2001) Generalised Modelling, Simulation and Control Design for Manipulators with Flexible Links and Flexible/Rigid Joints. Research Report. ACSE Research Report 806 . Department of Automatic Control and Systems Engineering

Reuse
Unless indicated otherwise, fulltext items are protected by copyright with all rights reserved. The copyright exception in section 29 of the Copyright, Designs and Patents Act 1988 allows the making of a single copy solely for the purpose of non-commercial research or private study within the limits of fair dealing. The publisher or other rights-holder may allow further reproduction and re-use of this version - refer to the White Rose Research Online record for this item. Where records identify the publisher as the copyright holder, users can verify any specific terms of use on the publisher's website.

Takedown
If you consider content in White Rose Research Online to be in breach of UK law, please notify us by emailing eprints@whiterose.ac.uk including the URL of the record and the reason for the withdrawal request.

White Rose
university consortium
Universities of Leeds, Sheffield & York

eprints@whiterose.ac.uk
https://eprints.whiterose.ac.uk/

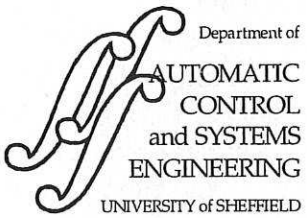

GENERALISED MODELLING, SIMULATION AND CONTROL DESIGN FOR MANIPULATORS WITH FLEXIBLE LINKS AND FLEXIBLE/RIGID JOINTS

B.Subudhi and A.S.Morris

Department of Automatic Control and Systems Engineering, The University of Sheffield, Mappin Street, Sheffield S1 3JD, UK.
E-mails: COQ98BS@sheffield.ac.uk,a.morris@sheffield.ac.uk

Research Report Number 806

October 2001

Abstract
In this paper, a generalised Euler-Lagrange assumed modes formulation for a manipulator with multiple flexible links and flexible joints is presented. The general modelling scheme is validated through computer simulations and analysis of the simplified single and two link manipulator models, with two different combinations of links and joints, namely first, flexible link(s) and rigid joints(s) and the second, flexible link(s) and flexible joint(s). To resolve the control complexity associated with the under-actuated flexible link and flexible joint manipulator, a singular perturbation model and control design for tracking are proposed with simultaneous suppression of the tip and joint vibrations.

Keywords: Manipulator, Flexible link, Flexible joint, Singular Perturbation

1. Introduction

Research on the dynamic modelling and control of flexible manipulators has received increased attention since the last thirty years due to their several advantages over rigid ones [1,2]. Unlike rigid manipulators, the dynamic models of this class of manipulators incorporate the effects of mechanical flexibilities in the links and joints. Link flexibility is a consequence of the lightweight constructional feature of manipulator arms that are designed to achieve low inertia for faster speeds. Similarly, joint flexibility arises because of the elastic behaviour of the joint transmission elements such as gears and shafts. Thus, flexible manipulators undergo two types of motion i.e. rigid and flexible motion. Because of the interaction of these motions, the resulting dynamic equations of flexible manipulators are highly complex and, in turn, the control task becomes more challenging compared to that for rigid robots. Therefore, a first step towards designing an efficient control strategy for these manipulators must be aimed at developing accurate dynamic models that can characterise the above flexibilities along with the rigid dynamics.

Investigations on modelling and control of flexible manipulators can be broadly classified into two categories, namely manipulators with flexible link(s) and manipulators with flexible joint(s). Although it is customary that the manipulators with flexibility in their links are known as flexible manipulators in literature, the latter group of manipulators which considers the links to be rigid but the joints to be flexible can also be categorised as flexible manipulators.

Much work has been reported on modelling of manipulators with flexible links and rigid joints using either the assumed mode method (AMM) [1,2,8] or the finite element method [14,15]. Because of the complexities involved in deriving dynamic models for multi-link flexible manipulators, most of the past work has only considered single-link cases. However, multi-link flexible manipulators are needed because a single link flexible robot is of little use in most practical applications.

Similarly, a number of researchers have addressed the modelling of a manipulator with joint flexibility. The dynamic behaviour of robotic manipulators with rigid links and flexible joints for both single and multi-link cases have been investigated in [5,12]. In these formulations, the elastic joints of the manipulators have been modelled as linear torsional springs and the manipulator dynamics have been described using the Lagrangian formulation.

Since it has been determined experimentally that joint flexibility exists in most manipulators in the drive transmission systems [13], the assumption of flexible links but rigid joints is invalid. Similarly, by considering joints to be flexible but the links to be rigid, the advantages of achieving more favourable payload to mass ratio of the arm, low power requirement and high speed etc. are sacrificed. Therefore, to satisfy the requirements for high speeds and good system performance, it is necessary to consider the dynamic effects of both link and joint flexibility. Recognising the above, coupling effects between a flexible link and flexible joint have been addressed in [4,7, 16-18]. Two models for a single-link manipulator with both link and joint flexibility have been derived using the Euler-Lagrange AMM, one with a set of decoupled equations and the other with a set of coupled equations [17]. In a similar work, Lin and Gogate [4] derived the dynamics of a manipulator with one flexible link and one flexible joint using the Hamiltonian AMM. Subsequently, Yang and Donath [18] extended their approach to develop a dynamic model of a two-link manipulator with link and joint flexibility. They reported that the elasticity in each joint adds an additional degree of freedom to the manipulator systems, which in turn results in a large variation in the dynamic behaviour of the manipulators. However, their model does not give clear insight into the mechanisms of

joint deflection and the effects of structural damping. Lin and Gogate [7] proposed a modelling scheme for a multi-link manipulator with both link and joint flexibility. However, they did not consider the effects of the payload and structural damping of the links in their model formulation. It has been shown that both the link and the joint flexibility need to be incorporated in the modelling to achieve good trajectory tracking and quick damping of end tip vibrations [7,17,18]. The flexible deformations produced by the joints and the links make it difficult for the end-effctor to track a prescribed trajectory accurately. Therefore, how to reduce the vibrations of the links and the joints is a significant concern. Studies on dynamic simulations of one-link and two-link robot manipulators with both link and joint flexibility have revealed that both the flexibilities need to be considered in the analysis and control of such manipulator systems [4,7,16-18]. Therefore, in this work, both the link flexibility and the joint flexibility are considered.

The modelling of the flexible link and joint manipulator described in this paper is different from that of [7] and [18] in several ways. First, it follows a systematic approach for deriving the dynamic equations for a *n*-link and *n*-joint manipulator which is accomplished by the use of two homogeneous transformation matrices describing the rigid and flexible motions respectively. Second, it also gives a clear picture of the joint deflection in terms of discrepancies between link and joint angles. Unlike the model derived by Lin and Gogate [7], the dynamic models of the manipulators in this paper consider the payload and the structural damping of the links.

The paper is organised as follows. In section 2, a generalised Euler-Lagrange AMM formulation for modelling of a manipulator with flexibilities in both links and joints is presented. Subsequently using this, the dynamic equations for a single-link manipulator with flexible link but rigid joint is derived in section 3. In following the generalized approach, closed-form dynamic models for a manipulator with single flexible link and joint are obtained in section 4. The development of dynamic equations for two-link flexible manipulators with rigid and flexible joints are dealt with in sections 5 and 6 respectively. Subsequently, a two-time-scale singularly perturbed model is proposed in section 7. Based on the two-time-scale separation of the flexible link and flexible joint manipulator dynamics, a controller is designed for tracking and control of tip and joint vibrations in section 8. Results corresponding to dynamic behaviour of the different flexible manipulators with bang-bang torque input(s) without any control actions along with performances achieved on employing the proposed controller are presented and discussed in section 9. The paper is concluded with a brief summary in section 10.

2. General Euler-Lagrange assumed modes formulation for modelling of multiple flexible links and flexible joints

2.1 Description of the Manipulator System

The structure of a multiple flexible links and flexible joints manipulator is shown in Fig.1. It consists of n flexible links and n flexible revolute joints. These links are cascaded in serial fashion and are actuated by rotors and hubs with individual motors. An inertial payload of mass M_P and inertia I_P is connected to the distal link. The proximal link is clamped and connected to the rotor with a hub.

2.2 Flexible Link and Flexible Joint Assembly

The schematic representation for the ith flexible joint and flexible link assembly is shown in Fig.2. The flexible joint is dynamically simplified as a linear torsional spring that works as a

connector between the rotor and the flexible link. α_i, θ_i are the ith rotor and link angular positions respectively. I_{ri} is the inertia of the ith rotor and hub, where an input torque, $\tau_i(t)$ is applied. G_i is the gear ratio for the ith rotor and k_{si} is the spring constant of the ith flexible link $(FJ)_i$.

2.3 Assumptions

The following assumptions are made for the development of a dynamic model of the flexible manipulator.

I. Each link is assumed to be long and slender. Therefore, transverse shear and the rotary inertia effects are negligible.

II. The motion of each link is assumed to be in the horizontal plane.

III. Links are considered to have constant cross-sectional area and uniform material properties.

IV. Each link is subjected to pure bending and its deflection is small.

V. Motion of the links can have deformations in the horizontal direction only.

VI. The kinetic energy of the rotor is mainly due to its rotation only and the rotor inertia is symmetric about its axis of rotation.

VII. The backlash of the reduction gear and coulomb friction effects are neglected.

2. 4 Kinematics Descriptions

In this section, the flexible link kinematics is described. Instead of just considering one or two-links [18], the kinematics description is given here for a chain of n serially connected flexible links. The co-ordinate systems of the link are assigned (Fig.1) referring to the Denavit-Hartenberg (D-H) description [3]. X_0Y_0 is the inertial co-ordinate frame (CF) and X_iY_i is the rigid body CF frame associated with the ith link and $\hat{X}_i\hat{Y}_i$ is the flexible moving CF.

Considering revolute joints and motion of the manipulator on a two-dimensional plane, the rigid transformation matrix, $\mathbf{A}_i$, from $X_{i-1}Y_{i-1}$ to X_iY_i is written as [3].

$$\mathbf{A}_i = \begin{bmatrix} cos\theta_i & -sin\theta_i \\ sin\theta_i & cos\theta_i \end{bmatrix} \tag{1}$$

On using assumption (IV), the elastic homogenous transformation matrix, $\mathbf{E}_i$, due to the deflection of the link i can be written as [2,8,14]:

$$\mathbf{E}_i = \begin{bmatrix} 1 & -\dfrac{\partial v_i(x_i,t)}{\partial x_i}\Big|x_i = l_i \\ \dfrac{\partial v_i(x_i,t)}{\partial x_i}\Big|x_i = l_i & 1 \end{bmatrix} \tag{2}$$

where $v_i(x_i,t)$ is the bending deflection of the ith link at a spatial point x_i $(0 \le x_i \le l_i)$ and l_i is the length of the ith link. The global transformation matrix, $\mathbf{T}_i$ transforms co-ordinates from X_0Y_0 to X_iY_i follows a recursion as below [2,8,14].

$$\mathbf{T_i} = \mathbf{T_{i-1}E_{i-1}A_i} = \hat{\mathbf{T}}_{\mathbf{i-1}}\mathbf{A}_i,\ \hat{\mathbf{T}}_{\mathbf{0}} = \mathbf{I} \tag{3}$$

Let ${}^{i}r_i(x_i) = \begin{Bmatrix} x_i \\ v_i(x_i,t) \end{Bmatrix}$ be the position vector that describes an arbitrary point along the ith deflected link with respect to its local CF (X_iY_i) and ${}^{0}r_i$ be the same point referred to X_0Y_0. The position of the origin of $X_{i+1}Y_{i+1}$ with respect to X_iY_i is given by

$$ {}^{i}p_{i+1} = {}^{i}r_i(l_i) \tag{4} $$

and ${}^{0}p_i$ is its absolute position with respect to X_0Y_0.

Using the global transformation matrix, ${}^{0}r_i$ and ${}^{0}p_i$ can be written as:

$$ \left.\begin{aligned} {}^{0}r_i &= {}^{0}p_i + \mathbf{T_i}\ {}^{i}r_i \\ {}^{0}p_{i+1} &= {}^{0}p_i + \mathbf{T_i}\ {}^{i}p_{i+1} \end{aligned}\right\} \tag{5} $$

2.5 Dynamic equations of motion

To derive the dynamic equations of the motion of the multiple flexible links and flexible joints manipulator, the total energy associated with the manipulator system needs to be computed using the kinematics for a n-links and n-joints system explained in section 2.4 (Fig.1). In the formulation of a model for a two-flexible links and joints manipulator, Yang and Donath [18] determined the different components of the energy associated with the first and second links separately. They assumed small angular rotation of the links in deriving the kinetic and potential energies due to the motion of the links. For a practical manipulator, this small angle motion assumption is invalid. Also, the approach becomes tedious for deriving equations for a manipulator with many links and joints. Therefore, the derivation of the dynamic equations of the multi-link flexible manipulator presented in this paper does not assume small angular rotation. Instead of adopting only the rigid transformation matrix and then incorporating the elastic deformation of the links [7], the use of rigid and elastic transformation matrices makes the development in this formulation more systematic and easy. Here, the total energy expressions of the multiple links and joints manipulator can be obtained from the ith link and ith rotor energy expressions directly.

The total kinetic energy of the manipulator (T) is given by

$$ T = T_R + T_L + T_{PL} \tag{6} $$

where T_R, T_L and T_{PL} are the kinetic energy associated with the rotors, links and the hubs respectively. Using assumption (VI), the kinetic energy of the ith rotor is given by

$$ T_{Ri} = \frac{1}{2}\ J_i \dot{\alpha}_i^2 \tag{7} $$

where $J_i = G_i^2 I_{ri}$, and $\dot{\alpha}_i$ is the angular velocity of the rotor about the ith principal axis. Therefore, the total kinetic energy for all the n rotors becomes

$$ T_R = \frac{1}{2}\ \dot{\boldsymbol{\alpha}}^T \mathbf{J}\, \dot{\boldsymbol{\alpha}} \tag{8} $$

where $\boldsymbol{\alpha} = \{\alpha_i\}$; $\mathbf{J} = diag(J_i)$; $i=1,2,...n$.

The kinetic energy of a point $r_i(x_i)$ on the ith link can be written as

$$ T_{Li} = \frac{1}{2}\rho_i \int_0^{l_i} {}^{0}\dot{r}_i^T(x_i)\, {}^{0}\dot{r}_i(x_i)\, dx_i \tag{9} $$

where ρ_i is the linear mass density for the ith link and ${}^{0}\dot{r}_i(x_i)$ is the velocity vector. The velocity vector can be computed by taking the time derivative of its position (5):

$$ {}^0\dot{r}_i(x_i) = {}^0\dot{p}_i + \dot{\mathbf{T}}_i\, {}^i r_i(x_i) + \mathbf{T}_i\, {}^i\dot{r}_i(x_i) \tag{10} $$

${}^0\dot{p}_i$ in (10) can be determined using (4,5) along with

$$ {}^i\dot{p}_{i+1} = {}^i\dot{r}_i(l_i) \tag{11} $$

The time derivative of the global transformation matrix $\dot{\mathbf{T}}_i$ can be recursively calculated from [2,8,14]

$$ \dot{\mathbf{T}}_i = \dot{\hat{\mathbf{T}}}_{i-1}\mathbf{A}_i + \hat{\mathbf{T}}_{i-1}\dot{\mathbf{A}}_i \;,\; \dot{\hat{\mathbf{T}}}_i = \mathbf{T}_i\mathbf{E}_i + \mathbf{T}_i\dot{\mathbf{E}}_i \tag{12} $$

Computation of $\dot{\mathbf{A}}_i$ and $\dot{\mathbf{E}}_i$ for (12) can be made as follows [8].

$$ \dot{\mathbf{A}}_i = \mathbf{S}\mathbf{A}_i\dot{\theta}_i \text{ and } \dot{\mathbf{E}}_i = \mathbf{S}\frac{\partial \dot{v}_i}{\partial x_i}\bigg|_{x_i=l_i} \quad \text{where } \mathbf{S} = \begin{bmatrix} 0 & -1 \\ 1 & 0 \end{bmatrix} \tag{13} $$

Evaluation of the transpose and derivative of transpose terms of the velocity vector in (9) can be easily accomplished by using the following identities [8]

$$ \mathbf{A}_i^{\mathrm{T}}\mathbf{A}_i = \mathbf{E}_i^{\mathrm{T}}\mathbf{E}_i = \mathbf{S}^{\mathrm{T}}\mathbf{S} + \mathbf{I} \text{ and } \mathbf{E}_i^{\mathrm{T}}\dot{\mathbf{E}}_i = (\mathbf{I}v_i'(l_i,t) + \mathbf{S})\dot{v}_i'(l_i,t) \tag{14} $$

$$ \mathbf{A}_i^{\mathrm{T}}\dot{\mathbf{A}}_i = \mathbf{S}\dot{\theta}_i \tag{15} $$

where $\mathbf{I}$ is the identity matrix of appropriate dimensions. After determining the kinetic energy associated with the ith link, the kinetic energy of all the n-links can be found as:

$$ T_L = \sum_{i=1}^{n}\frac{1}{2}\rho_i\int_0^{l_i}\dot{r}_i^T(x_i)\dot{r}_i(x_i)dx_i \tag{16} $$

Referring to Fig.1 and the kinematics described in section 2.4, the kinetic energy associated with the payload can be written as

$$ T_{PL} = \frac{1}{2}M_P\dot{p}_{n+1}^T\dot{p}_{n+1} + \frac{1}{2}I_P(\dot{\Omega}_n + \dot{v}_n'(l_n))^2 \tag{17} $$

where $\dot{\Omega}_n = \sum_{j=1}^{n}\dot{\theta}_j + \sum_{k=1}^{n-1}\dot{v}_k'(l_k)$; n being the link number, $(')$ and $\dot{()}$ represent the first derivatives with respect to spatial variable x and time respectively. $\dot{p}_{n+1}$ can be determined using (4,5).

Next, neglecting the effects of the gravity, the total potential energy of the system can be written as

$$ U = U_S + U_J \tag{18} $$

where U_S and U_J are the potential energy resulting from the elastic deflection of the links and joints respectively. The potential energy due to the deformation of the link i can be written as

$$ U_{Si} = \int_0^{l_i}(EI)_i\left(\frac{d^2v_i(x_i)}{dx_i^2}\right)dx_i \tag{19} $$

Therefore, for all the n-links it becomes

$$ U_S = \sum_i^n\frac{1}{2}\int_0^{l_i}(EI)_i\left(\frac{d^2v_i(x_i)}{dx_i^2}\right)dx_i \tag{20} $$

Let the deflection of the ith rotor be $(a_i - \theta_i)$. Then the elastic potential energy for the ith flexible joint can be written as

$$ U_{Ji} = \frac{1}{2}k_{si}(a_i - \theta_i)^2 \tag{21} $$

For n-flexible joints, the total elastic potential energy can be written in vector matrix notation as

$$U_J = \frac{1}{2}\mathbf{K}_s(\alpha-\theta)^T(\alpha-\theta) \tag{22}$$

where $(EI)_i$ is the flexural rigidity of the ith link; $\theta = \{\theta_i\}$, $i = 1,2...n$ and the stiffness matrix of the joint ($\mathbf{K}_s$) is written as

$$\mathbf{K}_s = diag(k_{si}) \tag{23}$$

In fact, each link possess some internal structural damping. The link damping is modelled with Rayleigh's dissipation function [9]. Using this, the dissipation energy for the ith link and jth mode can be written as

$$E_{Di} = \frac{1}{2}d_{ij}\dot{q}_{ij}^2 \tag{24}$$

Therefore for all the n-links, each with n_m modes, the total dissipative energy in vector and matrix form can be expressed as

$$E_D = \frac{1}{2}\dot{q}^T\mathbf{D}\dot{q}^T \tag{25}$$

where the damping matrix, $\mathbf{D} = \mathbf{diag}(d_{ij})$, $i = 1,2..n$; $j = 1,2,.....n_m$; n_m being the number of finite modes (to be explained later); d_{ij} is the damping coefficient and the modal displacement vector is $q = \{q_{ij}\}$

Using the assumption (I), the dynamics of the link at an arbitrary spatial point x_i along the link at instant of time t can be written using the Euler-Beam theory as [9]

$$(EI)_i\frac{\partial^4 v_i(x_i,t)}{\partial x_i^4} + \rho_i\frac{\partial^2 v_i(x_i,t)}{\partial t^2} = 0 \tag{26}$$

where ρ_i is the linear mass density of the ith link. Solution of (26) is accomplished with the boundary conditions of the manipulator. Considering a clamped-mass configuration of the manipulator, the boundary conditions can be written as [8,14]

$$v_i(x_i,t)\big|_{x_i=0} = 0 \tag{27}$$

$$v_i'(x_i,t)\big|_{x_i=0} = 0 \tag{28}$$

$$(EI)_i\frac{\partial^2 v_i(x_i,t)}{\partial x_i^2}\bigg|_{x_i=l_i} = -I_{E_i}\frac{d^2}{dt^2}\left(\frac{\partial v_i(x_i,t)}{\partial x_i}\bigg|_{x_i=l_i}\right) - (M_{DE_i}\frac{d^2}{dt^2}\left(\frac{\partial v_i(x_i,t)}{\partial x_i}\bigg|_{x_i=l_i}\right) \tag{29}$$

$$(EI)_i\frac{\partial^3 v_i(x_i,t)}{\partial x_i^3}\bigg|_{x_i=l_i} = M_{E_i}\frac{d^2}{dt^2}\left(v_i(x_i,t)\big|_{x_i=l_i}\right) + M_{DE_i}\frac{d^2}{dt^2}\left(v_i(x_i,t)\big|_{x_i=l_i}\right) \tag{30}$$

where M_{E_i}, I_{E_i} are the effective mass and moment of inertias at the end of the ith link and M_{D_i} is the contributions of masses of distal links. These are defined below.

$$M_{E_i} = \frac{M_{L_i}}{m_i},\ I_{E_i} = \frac{I_{L_i}}{m_i l_i},\ M_{DE_i} = \frac{M_{D_i}}{m_i l_i^2} \tag{31}$$

A finite dimensional solution of (21) can be obtained by means of AMM [9]. Using this method, $v_i(x_i,t)$ can be expressed as a superposition of mode-shapes and time dependent modal displacements,

$$v_i(x,t) = \sum_{j=1}^{n_m} \phi_{ji}(x_i) q_{ij}(t) \tag{32}$$

where $\phi_{ij}(x_i)$ and $q_{ij}(t)$ respectively are the jth mode shape function and jth modal displacement for the ith link. Substituting for $v_i(x,t)$ from (32) in (26) gives,

$$\frac{(EI)_i}{\rho\phi_{ij}(x_i)} \frac{d^4\phi_{ij}(x)}{dx_i^4} = -\frac{1}{q_{ij}(t)} \frac{d^2 q_{ij}(t)}{dt^2} = \omega_{ij}^{\ 2} \tag{33}$$

where the constant is ω_{ij}^2. Separating (2.33) into spatial and temporal parts yields,

$$\frac{d^2\left((EI)_i \dfrac{d^2\phi_{ij}}{dx_i^2}\right)}{dx_i^2} - \omega_{ij}^2 \rho \phi_{ij} = 0 \tag{34}$$

$$\frac{d^2 q_{ij}(t)}{dt^2} + \omega_{ij}^2 q_{ij}(t) = 0 \tag{35}$$

The time domain solution of (35) is

$$q_{ij}(t) = \exp(\omega_{ij} t) \tag{36}$$

and the solution of (34) is of the form

$$\phi_{ij}(x_i) = N_{ij}[(\cos(\beta_{ij} x_i) - \cosh(\beta_{ij} x_i) + \gamma_{ij} \sinh(\beta_{ij} x_i) - \cosh(\beta_{ij} x_i)] \tag{37}$$

γ_{ij} 's are given as [14]:

$$\gamma_{ij} = \frac{\sin\beta_{ij} - \sinh\beta_{ij} + M_{E_i}\beta_{ij}(\cos\beta_{ij} - \cosh\beta_{ij}) - M_{DE_i}\beta_{ij}^{\ 2}(\sin\beta_{ij} + \sinh\beta_{ij})}{\cos\beta_{ij} + \cosh\beta_{ij} - M_{E_i}\beta_{ij}(\sin\beta_{ij} - \sinh\beta_{ij}) - M_{DE_i}\beta_{ij}^{\ 2}(\cos\beta_{ij} - \cosh\beta_{ij})} \tag{38}$$

and β_{ij} 's are the solution of the following equation [8,14]

$$\begin{aligned} &1 + \cosh\beta_{ij} l_i \cos\beta_{ij} l_i - M_{E_i}\beta_{ij}(\sinh\beta_{ij} l_i - \cosh\beta_{ij} l_i \sin\beta_{ij} l_i) \\ &- I_{E_i}(\beta_{ij})^3(\sinh\beta_{ij} l_i + \cosh\beta_{ij} l_i \sin\beta_{ij} l_i) + M_{E_i} I_{E_i}(\beta_{ij})^4(1 - \cosh\beta_{ij} l_i \sin\beta_{ij} l_i) \\ &+ M_{DE_i}^{\ 2}(\beta_{ij})^4(1 - \cosh\beta_{ij} l_i \sin\beta_{ij} l_i) - 2M_{DE_i}^{\ 2}(\beta_{ij})^4 \sinh\beta_{ij} l_i = 0 \end{aligned} \tag{39}$$

N_{ij} 's are the constants that normalize the mode shape functions such that

$$N_{ij} = \int_o^{l_i} [\phi_{ij}(x_i)]^2 dx_i = m_i \tag{40}$$

where m_i is the mass of the link i. Subsequently, the natural frequency for the jth mode and ith link, ω_{ij}, is determined from the following expression

$$\beta_{ij}^4 = \frac{\omega_{ij}^2 \rho_i}{(EI)_i} \tag{41}$$

Next, to obtain a closed-form dynamic model of the manipulator, the above energy expressions (6-25) are used to formulate the Lagrangian $L = T - U$. Using the Euler-Lagrange equation

$$\frac{\partial}{\partial t}\left(\frac{\partial L}{\partial \dot{Q}_i}\right) - \frac{\partial L}{\partial Q_i} + \frac{\partial E_D}{\partial \dot{Q}_i} = F_i \tag{42}$$

with the ith generalised co-ordinate of the system, Q_i, and the corresponding generalised forces, F_i, a set of $(4n + 2n_m)$ numbers of differential equations are obtained. In (42), Q_i, and

F_i are defined as follows. $Q = \{Q_i\}$; $Q = \{\alpha \quad \theta \quad q\}^T$; $F = \{F_i\}$, $i = 1,2,.....,4n+2n_m$; $F = \{\tau \quad 0 \quad 0\}^T$; $\tau = \{\tau_i\}$ and $i = 1,2,.....4n+2n_m$. After mathematical simplification, these $(4n+2n_m)$ dynamic equations can be written in compact form as:

$$\mathbf{J}\ddot{\alpha} - \mathbf{K}_s(\theta - \alpha) = \tau \tag{43}$$

$$\mathbf{M}(\theta,q)\begin{Bmatrix}\ddot{\theta}\\ \ddot{q}\end{Bmatrix} + \begin{Bmatrix}f_1(\theta,\dot{\theta})\\ f_2(\theta,\dot{\theta})\end{Bmatrix} + \begin{Bmatrix}g_1(\theta,\dot{\theta},q,\dot{q})\\ g_2(\theta,\dot{\theta},q,\dot{q})\end{Bmatrix} + \begin{Bmatrix}0\\ \mathbf{D}\dot{q}\end{Bmatrix} + \begin{Bmatrix}\mathbf{K}_s(\theta-\alpha)\\ \mathbf{K}_w q\end{Bmatrix} = \begin{Bmatrix}0\\ 0\end{Bmatrix} \tag{44}$$

where $\mathbf{M}$ is the mass matrix, $\mathbf{J}$ is the modified rotor inertia matrix with its elements (J_i), $f_1(.)$ and $f_2(.)$ are the vectors containing terms due to Coriolis and Centrifugal forces, $g_1(.)$ and $g_2(.)$ are the vectors containing terms due to the interactions of the link angles and their rates with the modal displacements and their rates. The components of the above vectors are determined by using the Christoffel symbols as [3,8]

$$c^{fg}(.) = \sum_{j=1}^{2n+2n_m}\sum_{k=1}^{2n+2n_m}\left(\frac{\partial M_{ij}}{\partial Q_k^{fg}} - \frac{\partial M_{jk}}{\partial Q_i^{fg}}\right)\dot{Q}_j^{fg}\dot{Q}_k^{fg} \tag{45}$$

where $c^{fg}(.) = \begin{Bmatrix}f_1(.)\\ f_2(.)\end{Bmatrix} + \begin{Bmatrix}g_1(.)\\ g_2(.)\end{Bmatrix}$ and $Q^{fg} = \{Q_i^{fg}\}$, $i = 1,2,..2n+2n_m$. The stiffness matrix due to the distributed flexibility of the links is given by

$$\mathbf{K}_w = diag(k_{11}, k_{12}...k_{1n_m}, k_{21}, k_{22}.....k_{2n_m}) \qquad \text{where } k_{ij} = \omega_{ij}^2 m_i \tag{46}$$

3. Dynamic model of single-link flexible manipulator with rigid joint (Model I)

In this section, the simplest case of a dynamic model for a manipulator with one flexible link but rigid joint is derived first. Consider one flexible link and one rigid joint (Fig.1). In the derivation the suffix for the link and joint number are dropped for simplicity. To derive the dynamics of a single-link manipulator with only link flexibility, the energies are determined as follows.

Let $r(x) = \begin{Bmatrix}x\\ v(x,t)\end{Bmatrix}$ be the position vector that describes an arbitrary point along the deflected link with respect to its local CF, XY, and ${}^0r$ be the same point referred to X_0Y_0. Using (5), ${}^0r$ can be written as:

$${}^0r = \mathbf{T}_1 r \tag{47}$$

$$\mathbf{T}_1 = \mathbf{A}_1, \text{ as } \hat{\mathbf{T}}_0 = \mathbf{I} \tag{48}$$

By using (11) to (15), ${}^0\dot{r}$ can be determined as

$${}^0\dot{r} = \begin{bmatrix}cos\theta & -sin\theta\\ sin\theta & cos\theta\end{bmatrix}\begin{bmatrix}-v(x,t)\dot{\theta}\\ x\dot{\theta} + \dot{v}(x,t)\end{bmatrix} \tag{49}$$

The kinetic energy due to the motion of the link can be expressed as

$$T_L = \frac{1}{2}\rho\int_0^l {}^0\dot{r}^T\,{}^0\dot{r}\,dx \tag{50}$$

Substitution of ${}^0\dot{r}$ from (3) into (4) yields

$$T_L = \frac{1}{2}\rho\int_o^l [v^2(x,t)\dot{\theta}^2 + x^2\dot{\theta}^2 + \dot{v}^2(x,t) + 2x\dot{\theta}\dot{v}(x,t)]dx \tag{51}$$

Similarly, the kinetic energy associated with the payload can be found as

$$T_{PL} = \frac{1}{2} M_P \{ v^2(x,t)\big|_{x=l} \dot{\theta}^2 + l^2 \dot{\theta}^2 + \dot{v}^2(x,t)\big|_{x=l} + 2l\dot{\theta}\dot{v}(x,t)\big|_{x=l} \} \tag{52}$$

As the joint is considered to be rigid, the kinetic energy due to the motion of the rotor and hub can be written as

$$T_R = \frac{1}{2} I_r \dot{\theta}^2 \tag{53}$$

The total kinetic energy of the flexible manipulator system (T) is

$$T = T_L + T_R + T_{PL} \tag{54}$$

Next, as the joint flexibility is not considered and the effect of gravity is ignored according to assumption II, the total potential energy of the system (U) in the present case is only due to the strain energy of the link and can be written as

$$U = \frac{1}{2} \int_0^l EI \left(\frac{\partial^2 v(x,t)}{\partial x^2} \right)^2 dx \tag{55}$$

The dissipative energy due to structural damping of the links is given by

$$E_D = \frac{1}{2} \dot{\boldsymbol{q}}^T \mathbf{D} \dot{\boldsymbol{q}}^T \tag{56}$$

where $\mathbf{D} = diag(d_i)$, $i = 1,2...n_m$; d_i is the damping coefficient of the ith mode.

Using the general expression (37), the ith mode shape for the single-link manipulator with clamped-mass configuration can be written as

$$\phi_i(x) = N_i[(\cos(\beta_i x) - \cosh(\beta_i x) + \gamma_i \sinh(\beta_i x) - \cosh(\beta_i x)] \tag{57}$$

Setting $M_L = M_P$, $I_L = M_P l^2$ and $M_D = 0$ in (38) for the single-link case yields

$$\gamma_i = \frac{\sin \beta_i - \sinh \beta_i}{\cos \beta_i + \cosh \beta_i} \tag{58}$$

and from (39) the eigenvalues β_i's can be determined by solving the following transcendental equation

$$1 + \cosh \beta_i l \cos \beta_i l - M_E \beta_i (\sinh \beta_i l - \cosh \beta_i l \sin \beta_i l) = 0 \tag{59}$$

where $M_E = \frac{M_P}{m}$. N_i's are the normalisation constants of the mode shapes such that

$$N_i = \int_o^l [\phi_i(x)]^2 dx = m \tag{60}$$

Subsequently, the natural frequency for the ith mode, ω_i, is determined from the following expression

$$\beta_i^4 = \frac{\omega_i^2 \rho}{EI} \tag{61}$$

The dynamic equations of this manipulator on applying the Euler-Lagrange's equations with $\boldsymbol{Q} = [\theta \quad q_1 \quad q_2 \quad \cdots \quad q_{n_m}]^T$, $\boldsymbol{F} = \{\tau \quad 0 \quad 0 \quad 0 \quad \cdots \quad 0\}^T$ resulted in the following equations with $i = 1,2,..n_m$.

$$\frac{d}{dt}\left(\frac{\partial L}{\partial \theta} \right) - \frac{\partial L}{\partial \theta} = \tau \tag{62}$$

$$\frac{d}{dt}\left(\frac{\partial L}{\partial q_i} \right) - \frac{\partial L}{\partial q_i} + \left(\frac{\partial E_D}{\partial \dot{q}_i} \right) = 0 \tag{63}$$

After some algebraic manipulations, the closed-form dynamic equations for a single-link flexible manipulator with a rigid joint can be written as

$$\mathbf{M}\ddot{\boldsymbol{Q}} + \mathbf{C}\dot{\boldsymbol{Q}} + \mathbf{K}\boldsymbol{Q} = \boldsymbol{F} \tag{64}$$

4. Dynamic model for a single flexible link and flexible joint manipulator (Model II)

In this section, dynamic equations for a single-link manipulator are derived considering both the link and joint flexibility so that the resulting model can be used to study the effect of the joint flexibility on the manipulator dynamics and provide a basis for designing a suitable control scheme. The manipulator considered in this section is similar to that discussed in section 3, but here the joint is considered to be flexible rather than rigid.

Using the same concept for determining the kinetic energy of the rotor, T_R, as explained before, we can write

$$T_R = \frac{1}{2} J \dot{\alpha}^2 \qquad \text{where } J = G^2 I_r \tag{65}$$

Also the expressions for T_L and T_{PL} are the same as determined in section 3. Therefore, the total kinetic energy of the flexible manipulator system (T) can be determined using

$$T = T_L + T_R + T_{PL} \tag{66}$$

Next, the total potential energy of the system can be written as

$$U = U_S + U_J \tag{67}$$

where U_S is the same as expressed by equation (55) in section 3. To determine, the potential energy due to the deflection of the joint, U_J, we can follow the derivation presented in section 2, giving:

$$U_j = \frac{1}{2} k_s (\alpha - \theta)^2 \tag{68}$$

The damping energy of the link is the same as in (56). For the discretization of the link flexible dynamics, the same technique as detailed through (57) to (61) can be used. Therefore, the closed-form equations of motion of the manipulator can be obtained using the Euler-Lagrange's AMM with $\boldsymbol{Q} = [\alpha \quad \theta \quad q_1 \quad q_2 \quad \cdots \quad q_{nm}]^T$ and $\boldsymbol{F} = [\tau \quad 0 \quad 0 \quad 0 \quad \cdots \quad 0]^T$. Expanding the Lagrange's equation for different components of Q_i and F_i (with i=1,2.. n_m) yields:

$$\frac{d}{dt}\left(\frac{\partial L}{\partial \alpha}\right) - \frac{\partial L}{\partial \alpha} = \tau \tag{69}$$

$$\frac{d}{dt}\left(\frac{\partial L}{\partial \theta}\right) - \frac{\partial L}{\partial \theta} = 0 \tag{70}$$

$$\frac{d}{dt}\left(\frac{\partial L}{\partial q_i}\right) - \frac{\partial L}{\partial q_i} + \frac{\partial E_D}{\partial \dot{q}_i} = 0 \tag{71}$$

After simplification the resulting equations can be written concisely as

$$\mathbf{M}\ddot{\boldsymbol{Q}} + \mathbf{C}\dot{\boldsymbol{Q}} + \mathbf{K}\boldsymbol{Q} = \boldsymbol{F} \tag{72}$$

5. Modelling of a manipulator with two flexible links and two rigid joints (Model III)

In the preceding two sections, the manipulator models derived had one flexible link and one joint (either rigid or flexible). However, a single-link manipulator has limited practical use.

Therefore, this section and section 6 derive dynamic equations for a manipulator with two flexible links and two rigid joints.

Referring to Fig.1 consider two flexible links and rigid joints (in place of flexible joints). Let the first link be clamped and a payload be connected to the tip of the second link. To develop a simplified model with reasonable accuracy, consider two flexible modes to characterise the link deflections for each of the links ($n_m = 2$). This is valid as the first few modes are dominant compared to the higher modes. Referring to the derivations in section 2, the kinetic energy of the links (i =1,2) and the payload are calculated using (9) to (17). Assuming no flexibility in the joint, the kinetic energy associated with the ith rotor and hub can be written as

$$T_{Ri} = \frac{1}{2}\ I_{ri}\dot{\theta}_i^2 \tag{73}$$

Therefore, the total kinetic energy for the two rotors and hubs becomes

$$T_R = \frac{1}{2}\ \dot{\boldsymbol{\theta}}^T \mathbf{J}\,\dot{\boldsymbol{\theta}} \tag{74}$$

where $\mathbf{J} = diag(I_{ri})$; $i=1,2,...n.$

Therefore, the total kinetic energy (T) becomes

$$T = T_L + T_R + T_{PL} \tag{75}$$

In the similar way to the derivations in section 2, the total potential energy (in this case only the strain energy of the links, therefore, $U = U_s$) can be written as

$$U_s = \sum_i^2 \frac{1}{2}\int_0^{l_i} (EI)_i \left(\frac{d^2 v_i(x_i)}{dx_i^2}\right) dx_i \tag{76}$$

Also the energy due to structural damping of the links of the manipulator can be determined as

$$E_D = \frac{1}{2}\dot{\boldsymbol{q}}^T \mathbf{D}\dot{\boldsymbol{q}}^T \tag{77}$$

where the damping matrix, $\mathbf{D} = \mathbf{diag}(d_{ij})$, $i = 1,2$; $j = 1,2$; d_{ij} is the damping coefficient, and the modal displacement vector is $\boldsymbol{q} = \{q_{ij}\}$

The solution of the equation for the motion of the two flexible links and two rigid joints manipulator with clamped-mass boundary conditions can be obtained using the general procedures given in section 2, equations (26) to (41). In this case, the effective mass and inertias for the links are given below.

$$\left.\begin{aligned} M_{E_1} &= m_2 + M_P \\ I_{E_1} &= I_{b2} + I_{r2} + I_P + M_P l^2 \\ M_{D_1} &= (m_2 l_{c2} + M_P l_2 \cos\theta_2) \end{aligned}\right\} \tag{78}$$

where l_{c2} centre of mass of link 2.

$$M_{E_2} = M_P;\ I_{E_2} = I_P + M_P l^2 \text{ and } M_{D_2} = 0 \tag{79}$$

Dynamic equations of a two flexible links and two rigid joints manipulator are derived using the Lagrange's equation (34) with the generalised co-ordinates, $\boldsymbol{Q}$, consisting of the rotor angles, link angles and the deflection variables given by $\boldsymbol{Q} = [\theta_1 \quad \theta_2 \quad q_{11} \quad q_{12} \quad q_{21} \quad q_{22}]^T$

and the corresponding vector of generalised forces, $\boldsymbol{F} = [\tau_1 \quad \tau_2 \quad 0 \quad 0 \quad \cdot \quad \cdot \quad \cdot \quad 0]^T$, τ_1 and τ_2 are the torque applied by the rotor 1 and rotor 2 respectively. Therefore, the following Lagrange's equations are obtained with i=1,2 and j=1,2.

$$\frac{d}{dt}\left(\frac{\partial L}{\partial \dot{\theta}_i}\right) - \frac{\partial L}{\partial \theta_i} = \tau_i \tag{80}$$

$$\frac{d}{dt}\left(\frac{\partial L}{\partial \dot{q}_{1j}}\right) - \frac{\partial L}{\partial q_{1j}} + \frac{\partial E_D}{\partial \dot{q}_{1j}} = 0 \tag{81}$$

$$\frac{d}{dt}\left(\frac{\partial L}{\partial \dot{q}_{2j}}\right) - \frac{\partial L}{\partial q_{2j}} + \frac{\partial E_D}{\partial \dot{q}_{2j}} = 0 \tag{82}$$

After some mathematical manipulations, the final dynamic equations of motion of the manipulator can be written in compact form as:

$$\mathbf{M}_{6\times6}(Q)\ddot{Q}_{6\times6} + \begin{Bmatrix} f_1(\theta,\dot{\theta})_{2\times1} \\ f_2(\theta,\dot{\theta})_{4\times1} \end{Bmatrix}_{6\times1} + \begin{Bmatrix} g_1(\theta,\dot{\theta},q,\dot{q})_{2\times1} \\ g_2(\theta,\dot{\theta},q,\dot{q})_{4\times1} \end{Bmatrix}_{6\times1} + \begin{Bmatrix} 0 \\ \mathbf{D}_{4\times4}\,\dot{q} \end{Bmatrix} + \begin{Bmatrix} 0 \\ \mathbf{K}_{w\,4\times4}\,q \end{Bmatrix} = \begin{Bmatrix} \tau \\ 0 \end{Bmatrix} \tag{83}$$

$$\mathbf{K}_w = diag(k_{11}, k_{12}, k_{21}, k_{22}) \tag{84}$$

6. Dynamic model of a manipulator with two flexible links and joints (Model IV)

The next model of interest is the manipulator with two flexible links and flexible joints. This is presented in this section and will be used for study of the elastic behaviour of the joints in the link flexible motion. Consider two units of the n-link and n-joint manipulator (Fig.1) with the first one clamped and a payload connected to the tip of the second link. The resulting dynamic model can be exploited in devising control algorithms for this class of manipulator when there is flexibility in both links and joints. With a view to obtaining a simplified model with reasonable accuracy, two modes per link are considered i.e. $j = 1,2...n_m$ with $n_m = 2$.

To derive the kinetic, potential and the dissipative energies associated with the manipulator, we follow the procedure adopted in section 2. All these energy expressions can be obtained using (6) to (25) by substituting for links (i =1,2), for two joints (i =1,2) and for two modes (j=1,2).

The solution of the partial differential equation describing the flexible motion of the manipulator can be obtained following the general procedures given in (21) to (35). In this case the effective mass at the end of the individual links are set as

$$M_{E_1} = m_2 + M_P;\; I_{E_1} = I_{b2} + J_2 + I_P + M_P l^2;\; M_{DE_1} = (m_2 l_{c2} + M_P l_2 \cos\theta_2) \tag{85}$$

$$M_{E_2} = M_P;\; I_{E_2} = I_P + M_P l^2 \text{ and } M_{D_2} = 0 \tag{86}$$

Here, the generalised co-ordinate vector consists of rotor positions (α_1, α_2), link positions (θ_1, θ_2) and modal displacements $(q_{11}, q_{12}, q_{21}, q_{22})$. The generalised force vector is $\boldsymbol{F} = \{\tau_1 \quad \tau_2 \quad 0 \quad 0 \quad \cdot \quad \cdot \quad \cdot \quad 0\}^T$, where τ_1, τ_2 are respectively the torques applied by the rotor 1 and rotor 2. Therefore, the following Euler-Lagrange's equations result, with i=1 and 2 and j=1 and 2.

$$\frac{d}{dt}\left(\frac{\partial L}{\partial \dot{\alpha}_i}\right) - \frac{\partial L}{\partial \alpha_i} = \tau_i \tag{87}$$

$$\frac{d}{dt}\left(\frac{\partial L}{\partial \dot{\theta}_i}\right)-\frac{\partial L}{\partial \theta_i}=0 \tag{88}$$

$$\frac{d}{dt}\left(\frac{\partial L}{\partial \dot{q}_{1j}}\right)-\frac{\partial L}{\partial q_{1j}}+\frac{\partial E_D}{\partial \dot{q}_{1j}}=0 \tag{89}$$

$$\frac{d}{dt}\left(\frac{\partial L}{\partial \dot{q}_{2j}}\right)-\frac{\partial L}{\partial q_{2j}}+\frac{\partial E_D}{\partial \dot{q}_{2j}}=0 \tag{90}$$

The final dynamic equations of motion of the manipulator after algebraic simplifications can be put in concise form as:

$$\mathbf{J}_{2\times 2}\ddot{\alpha}-\mathbf{K}_{s2\times 2}(\theta-\alpha)=\tau \tag{91}$$

$$\mathbf{M}_{6\times 6}(\theta,q)\begin{Bmatrix}\ddot{\theta}\\ \ddot{q}\end{Bmatrix}+\begin{Bmatrix}f_1(\theta,\dot{\theta})\\ f_2(\theta,\dot{\theta})\end{Bmatrix}_{6\times 1}+\begin{Bmatrix}g_1(\theta,\dot{\theta},q,\dot{q})\\ g_2(\theta,\dot{\theta},q,\dot{q})\end{Bmatrix}_{6\times 1}+\begin{Bmatrix}0\\ \mathbf{D}_{4\times 4}\dot{q}\end{Bmatrix}+\begin{Bmatrix}\mathbf{K}_{s2\times 2}(\theta-\alpha)\\ \mathbf{K}_{w2\times 2}q\end{Bmatrix}=\begin{Bmatrix}0\\ 0\end{Bmatrix} \tag{92}$$

7. Two-time-scale singular perturbation model of a flexible link and flexible joint manipulator (FLFJM)

Control of flexible link manipulators is difficult because they are under-actuated systems in which all modes of flexure in each link have to be controlled by adjusting a single actuating torque. This difficulty is accentuated in the case where both the links and joints are flexible since the actuating torque for each link then has to control the flexure of both the link and its corresponding joint. A successful solution to this control problem in such under-actuated systems has been accomplished previously by using the singular perturbation technique [5,6,11]. This essentially uses a perturbation parameter to divide the complex dynamic systems into simpler subsystems at different time scales and has been successfully applied for controlling manipulators with either flexible links or flexible joints [5,11]. Therefore, in this work, the technique is utilised to obtain a singularly perturbed model for a manipulator where there is flexibility in both links and joints.

To formulate a two-time-scale singular perturbation model, we proceed as follows. Substituting $\delta=(\alpha-\theta)$ in (91,92), gives:

$$\mathbf{J}\ddot{\alpha}+\mathbf{K}_s\delta=\tau \tag{93}$$

$$\mathbf{M}(\theta,q)\begin{Bmatrix}\theta\\ q\end{Bmatrix}+\begin{Bmatrix}f_1(\theta,\dot{\theta})\\ f_2(\theta,\dot{\theta})\end{Bmatrix}+\begin{Bmatrix}g_1(\theta,\dot{\theta},q,\dot{q})\\ g_2(\theta,\dot{\theta},q,\dot{q})\end{Bmatrix}+\begin{Bmatrix}0\\ \mathbf{D}\dot{q}\end{Bmatrix}+\begin{Bmatrix}\mathbf{K}_s\delta\\ \mathbf{K}_w q\end{Bmatrix}=\begin{Bmatrix}0\\ 0\end{Bmatrix} \tag{94}$$

As the inertia matrix, $\mathbf{M}(.)$ is a positive definite, its inverse, $\mathbf{H}(.)$ can be partitioned. Hence, $\ddot{\theta}$ and $\ddot{q}$ can be determined as follows.

$$\begin{aligned}\ddot{\theta}=&-\mathbf{H}_{11}(.)f_1(.)-\mathbf{H}_{11}(.)g_1(.)-\mathbf{H}_{12}(.)g_2(.)-\mathbf{H}_{12}(.)f_2(.)\\&+\mathbf{H}_{11}(.)\mathbf{K}_s\delta-\mathbf{H}_{12}(.)K_w q-\mathbf{H}_{12}(.)\mathbf{D}\dot{q}\end{aligned} \tag{95}$$

$$\begin{aligned}\ddot{q}=&-\mathbf{H}_{21}(.)f_1(.)-\mathbf{H}_{21}(.)g_1(.)-\mathbf{H}_{22}(.)f_2(.)-\mathbf{H}_{22}(.)g_2(.)\\&-\mathbf{H}_{22}(.)\mathbf{K}_w q+\mathbf{H}_{21}(.)\mathbf{K}_s\delta-\mathbf{H}_{22}(.)\mathbf{D}\dot{q}\end{aligned} \tag{96}$$

Subtracting $\mathbf{J}\ddot{\theta}$ from both the sides of (91), we can write,

$$\ddot{\delta}=\ddot{\alpha}-\ddot{\theta}=-\mathbf{J}^{-1}\mathbf{K}_s\delta+\mathbf{J}^{-1}\tau-\ddot{\theta} \tag{97}$$

Now, define a common scale factor k_c, which is the minimum of all the stiffness constants, i.e. $k_c=\min(k_{11},k_{12},k_{21},k_{22},k_{s1},k_{s2})$. With this common scale factor, $\mathbf{K}_s$ and $\mathbf{K}_w$ can be

scaled by k_c such that, $\tilde{\mathbf{K}}_s = \frac{1}{k_c}\mathbf{K}_s$ and $\tilde{\mathbf{K}}_w = \frac{1}{k_c}\mathbf{K}_w$. Defining $\xi_q = k_c q$, $\xi_\delta = k_c \delta$, $\mu = \frac{1}{k_c}$ and substituting, $q = \mu\xi_q$ and $\delta = \mu\xi_\delta$ into (95-97), we get,

$$\ddot{\theta} = -\mathbf{H}_{11}(\theta,\mu\xi_q)f_1(\theta,\dot{\theta}) - \mathbf{H}_{11}(\theta,\mu\xi_q)g_1(\theta,\dot{\theta},) - \mathbf{H}_{12}(\theta,\mu\xi_q)g_2(\theta,\dot{\theta},\mu\xi_q,\mu\dot{\xi}_q) - \mathbf{H}_{12}(\theta,\mu\xi_q)f_2(\theta,\dot{\theta}) + \mathbf{H}_{11}(\theta,\mu\xi_q)\mathbf{K}_s\delta - \mathbf{H}_{12}(\theta,\mu\xi_q)\mathbf{K}_w q - \mathbf{H}_{12}(\theta,\mu\xi_q)\mathbf{D}\dot{q} \quad (98)$$

$$\mu\ddot{\xi}_q = -\mathbf{H}_{21}(\theta,\mu\xi_q)f_1(\theta,\dot{\theta}) - \mathbf{H}_{21}(\theta,\mu\xi_q)g_1(\theta,\dot{\theta},) - \mathbf{H}_{21}(\theta,\mu\xi_q)g_2(\theta,\dot{\theta},\mu\xi_q,\mu\dot{\xi}_q) - \mathbf{H}_{22}(\theta,\mu\xi_q)f_2(\theta,\dot{\theta}) + \mathbf{H}_{21}(\theta,\mu\xi_q)\mathbf{K}_s\delta - \mathbf{H}_{22}(\theta,\mu\xi_q)\mathbf{K}_w q - \mathbf{H}_{22}(\theta,\mu\xi_q)\mathbf{D}\dot{q} \quad (99)$$

$$\mu\xi_\delta = -J^{-1}\tilde{K}_s\,\xi_\delta + J^{-1}\tau - \ddot{\theta} \quad (100)$$

To derive the boundary layer correction, μ is set to zero [6] in (98) to (100) and on solving for $\bar{\xi}_q$ and $\bar{\xi}_\delta$ yields

$$\bar{\xi}_\delta = \tilde{\mathbf{K}}_s^{-1}(\bar{\tau} - \mathbf{J}\ddot{\bar{\theta}}) \quad (101)$$

$$\bar{\xi}_q = \tilde{\mathbf{K}}_w^{-1}\mathbf{H}_{22}^{-1}[-\mathbf{H}_{21}(\bar{\theta},0)f_1(\bar{\theta},\dot{\bar{\theta}}) - \mathbf{H}_{22}(\bar{\theta},0)f_2(\bar{\theta},\dot{\bar{\theta}}) - \mathbf{H}_{21}(\bar{\theta},0)(\bar{\tau} - \mathbf{J}\ddot{\bar{\theta}})] \quad (102)$$

where overbar denotes the value of a variable at $\mu = 0$. Applying the two-time-scale perturbation technique [5,6,11], the slow and fast subsystems can be obtained as follows.

Slow Subsystem:

$$\ddot{\bar{\theta}} = (\mathbf{M}_{11} + \mathbf{J})^{-1} \times [-f_1(\bar{\theta},\dot{\bar{\theta}}) + (\bar{\tau} - \mathbf{J}\ddot{\bar{\theta}})] \quad (103)$$

Fast Subsystem at a fast time scale, $t_f = \frac{t}{\varepsilon}$ *with* $\varepsilon = \sqrt{\mu}$ *:*

$$\dot{x}_f = \mathbf{A}_f x_f + \mathbf{B}_f \tau_f \quad (104)$$

where $\mathbf{A}_f = \begin{bmatrix} \mathbf{0} & \mathbf{0} & \mathbf{I} \\ -\mathbf{H}_{22}\tilde{\mathbf{K}}_w & \mathbf{H}_{21}\tilde{\mathbf{K}}_s & \mathbf{0} \\ \mathbf{0} & \mathbf{J}^{-1}\tilde{\mathbf{K}}_s & \mathbf{0} \end{bmatrix}$, $\mathbf{B}_f = \begin{bmatrix} \mathbf{0} \\ \mathbf{J}^{-1}\tilde{\mathbf{K}}_s \end{bmatrix}$; $x_f = [\eta_q^1 \quad \eta_a^1 \quad \eta_q^2 \quad \eta_a^2]^T$,

$n_q^1 = \xi_q - \bar{\xi}_q$; $n_q^2 = \varepsilon\dot{\xi}_q$; $n_a^1 = \xi_\delta - \bar{\xi}_\delta$; $n_a^2 = \varepsilon\dot{\xi}_\delta$, $\mathbf{0}$ and $\mathbf{I}$ matrices are of appropriate dimensions.

8. Design of composite control scheme

Fig. 3 gives the structure for the composite controller based on the two-time-scale model of the manipulator with two flexible links and two flexible joints given in (91,92). Following the composite control strategy, the net torque, τ can be determined as [6,11]

$$\tau = \bar{\tau} + \tau_f \quad (105)$$

where $\bar{\tau}$ is the slow control and τ_f is the fast control respectively. The controller for the slow subsystem can be designed according to computed torque control technique, which can be written as:

$$\bar{\tau} = (\mathbf{M}_{11} + \mathbf{J})\{\ddot{\theta}_d(t) + \mathbf{K}_{ps}(\theta_d(t) - \bar{\theta}(t)) + \mathbf{K}_{vs}(\dot{\theta}_d(t) - \dot{\bar{\theta}}(t))\} \quad (106)$$

where $\mathbf{K}_{ps}$ and $\mathbf{K}_{vs}$ are the diagonal position and velocity gain matrices of the controller and $\theta_d(t)$ are the desired trajectories of the two links. As the fast subsystem (104) is completely controllable, a fast state feedback control can be devised to force its states x_f to zero. This is given by:

$$\tau_f = \mathbf{K}_{pf} x_f + \mathbf{K}_{vf} \frac{dx_f}{dt_f} \tag{107}$$

where the feedback gains $\mathbf{K}_{pf}$ and $\mathbf{K}_{vf}$ are obtained through optimising the cost function using an LQR approach [10].

9. Implementation, results and discussions

The dynamic equations characterising the behaviours of different types of flexible manipulators derived in sections (3-6) are verified in this section. Equations describing the models (I-IV) were simulated using the fourth-order Runge-Kutta integration method at a sampling rate of 1ms. The physical parameters assumed for the single-link flexible manipulator (models I and II) are the same as used in [4] and are given in Table 1. In the case of the flexible link and flexible joint manipulator, the gear ratio, G, and the spring constant, k_s of the joint were taken as 10 and 100 Nm/rad respectively.

Models I and II were excited by a symmetric bang-bang torque input of 2 Nm and of 0.5second duration as shown in Fig.4(a). The responses of these models are given in Figs. 4 and 5. The link angular position response for model I (Fig.5(a)) is smooth, unlike the response of the flexible manipulator with joint flexibility (Model III, Fig. 4(b)) where a substantial amount of joint deflection (the difference between the rotor and link angular positions) exists in the manipulator drive systems. Figs. 4(c), 5(b) and 5(c) show the first and second modes of vibration curves for models I and II. It is evident that oscillations die out quickly for model I but increase in time for model II. This difference is confirmed by observation of the corresponding tip deflection responses in Figs. 4(d) and 5(d). It is clear that joint flexibility excites oscillatory behaviour in the link angular position. Thus, it is apparent that a control torque is needed to damp the joint deflection, the elastic modes of vibrations and the tip deflection.

Next, the manipulators with two-flexible links and two-joints (rigid or flexible) were studied. The physical parameters of models III and IV were taken from [8] and are given in Table 2. Both the links and rotors are considered to have the same dimensions. The gear ratio (G) and stiffness constant (k_s) of the flexible joints for Model IV were taken as 10 and 100 Nm/rad respectively. The manipulator dynamic equations for models III and IV were simulated with symmetric bang-bang torque inputs each of 0.2 Nm amplitude and 0.5 sec width applied at the rotors (see Fig.6(a)). The responses of Models III and IV to these torque inputs are presented in Figs. (6-9). It is observed from Fig. 6(b) and Fig. 7(a) that, in the case of model IV (with flexible joints), the angular position of the first link is more oscillatory than the second link. But, both the link position responses are not smooth. Also, these figures show that both the link angular positions have deviations from their respective rotor positions. Figs. 8(a) and 9(a) show that the bang-bang torque excitation causes less oscillation in the link angular positions of Model III (without joint flexibility) as compared to those with Model IV. The amplitudes of the first and second modes of vibrations for both the links in the case of Model IV (Figs. 6(c), 7(b), 7(c)) and the tip deflections of the links (Figs. 6(d) and 7(d)) are greater compared to the corresponding responses of Model III (Figs.8(b)-8(d) and 9(b)-9(d)). Also, the first and second modes of vibration of both the links are less excited in the case of the rigid joint manipulator (Model III), thereby causing the tip deflections to be well damped (Figs.8(b), 8(c), 8(d), 9(b), 9(b) and 9(d)). The oscillations in modal vibrations and tip deflections of Model IV do not decay with time, unlike the modes of vibration and the tip deflection responses of Model III. Thus, it is clear that joint flexibility significantly affects the link vibrations.

The tracking performance of the singular perturbation based composite controller applied to a manipulator with two flexible links and two flexible joints was verified considering the desired trajectories as

$$\theta_d(t) = \theta_0(t) + (6\frac{t^5}{t_d^5} - 15\frac{t^4}{t_d^4} + 10\frac{t^3}{t_d^3})(\theta_f - \theta_0) \tag{112}$$

where $\theta_d(t) = [\theta_{d1}(t) \quad \theta_{d2}(t)]^T$, $\theta_0 = [0 \quad 0]^T$ are the initial positions of the links, $\theta_f = \begin{bmatrix} \frac{\pi}{2} & \frac{\pi}{6} \end{bmatrix}$ are the final positions, t_d is the time taken to reach the final position which is taken as 2 seconds. The gains for the slow and fast control components of the composite singular perturbation control are obtained as $\mathbf{K}_{ps} = diag(5.0, 5.0)$; $\mathbf{K}_{vs} = diag(2.0, 2.0)$;

$\mathbf{K}_{pf} = \begin{bmatrix} 4.0 & 2.5 & -1.3 & 1.8 & 28.3 & -58.26 \\ 0.0 & -1.0 & -1.0 & 0.0 & 5.6 & 8.6 \end{bmatrix}$, $\mathbf{K}_{vf} = \begin{bmatrix} 8.0 & -37.2 & -1.5 & 28.8 & 126.0 & 58.03 \\ 4.0 & 0.0 & 5.0 & -3.0 & -8.6 & 14.7 \end{bmatrix}$.

The controller performances are shown in Figs. 10 and 11. It can be seen from Fig. 10(a) that good tracking performance is achieved through the application of the proposed controller. Figs. 10(c), 10(d) and 11(a), 11(b) show that first and second mode of vibration of both the links are well damped. The tip and joint deflections are also suppressed effectively while tracking the desired trajectories (see, Figs. 10(b), 11(c)). The control signals generated for the rotor 1 and rotor 2 using the composite controller are shown in Fig. 11(d).

10. Conclusions

A generalised modelling framework has been described to obtain the closed-form dynamic equations of motion for a multi-link manipulator considering flexibility in the links and the joints using the Euler-Lagrange assumed modes approach. Unlike the models derived in [18], the model presented for a multi-link manipulator with both link and joint flexibility is a generalised one. This is quite useful for the study of manipulators with many links and joints that are all flexible. As compared to the model formulation in [7], the proposed model is complete in the sense that it considers the effects of payload and structural damping of the links. It also provides a generalized model of a manipulator with both link and joint flexibility described by a set of closed-form differential equations satisfying the requirements for controller implementation. The general model formulation has been exploited to obtain the closed-form dynamic models for single and two link flexible manipulators. The model equations have been verified using bang-bang torque inputs, and model responses have been discussed. The two-time-scale separation of the complex dynamics of the flexible link and flexible joint manipulator makes the control design simpler. With application of the proposed controller to a flexible link and flexible joint manipulator, good tracking is performed and both link and joint vibrations are suppressed effectively.

References

[1] W.J. Book, Controlled, motion in an elastic world, Trans. ASME Journal of Dynamic Systems, Measurement, and Control, 115 (1993) 252-261.

[2] W.J. Book, Recursive Lagrangian dynamics of flexible manipulator arms, International Journal of Robotics Research, 3(3) (1984) 87-101.

[3] J.Denavit and R.S.Hartenburg, A kinematic notation for lower pair Mechanism based on Matrices, Journal of Applied Mechanics, 77 (1955) 215-221.

[4] S.Gogate and Y.J.Lin, Formulation and control of robots with link and joint flexibility, Robotica, 11, (1993) 273-142.

[5] K.Khorasani, Adaptive control of flexible joint-robots, IEEE Trans. on Robotics and Automation, 8(2), (1992) 251-267.

[6] P.V. Kokotovic, H.K.Khalil and J.O'Reilly, Singular perturbation methods in control: analysis and design, SIAM Classics in Applied Mathematics, USA, vol.25, 1999.

[7] Lin, Y.J. and Gogate, S.D., Modelling and motion simulation of an n-link flexible robot with elastic joints, in: Proceedings of the International Symposium on Robotics and Manufacturing, Santa Barbara, CA, 1989, pp.39-43.

[8] A.D.Luca and Brune Siciliano, Closed-form dynamic model of planar multi-link lightweight robots, IEEE Trans. Systems, Man, and Cybernetics, 21(4) (1991) 826-839.

[9] L.Meirovitch, Analytical Methods in Vibration, Macmillan Publ., Newyork, 1967.

[10] Katsuhiko Ogata, Modern Control Engineering, Upper Saddle River, New Jersey: Prentice Hall International, 1997.

[11] Brune Siciliano and W.J. Book, A Singular Perturbation Approach to Control of Lightweight Flexible Manipulators, International Journal of Robotics Research, 7(4) (1988) 79-90.

[12] M.W. Spong, Modelling and control of elastic joint robots, Trans. ASME Dynamic Systems, Measurement and Control, 109 (1987) 311-318.

[13] L.M.Sweet, and M.C.Good, Re-definition of the robot motion control problem: Effects of plant dynamics, Drive systems, constraints and user requirement, in: Proceedings of the 23rd IEEE Conference on Decision and Control, Las Vegas, 1984, pp.724-731.

[14] R.Theodore, and A.Ghosal, Comparison of the assumed modes and finite element models for flexible multi-link manipulators, Intl. Journal of Robotics Research, 1996, 14 (2) (1995) 91-111.

[15] P.B.Usoro, R.Nadira and S.S.Mahil, A finite element/Lagrange approach to modelling lightweight flexible manipulators, Trans. ASME Dynamic Systems, Measurement and Control, 108, (1986) 198-205.

[16] F. Xi, R. G.Fenton and B.Tabarrok, Coupling effects in a manipulator with flexible link and joints, Trans. ASME Dynamic Systems, Measurement and Control, 116, (1994) 827-831.

[17] G.B. Yang and M.Donath, Dynamic model of a one-link robot manipulator with both structural and joint flexibility, in: Proceedings of the IEEE Intl. Conf. on Robotics and Automation, Philadelphia, 1988, pp. 476-481.

[18] G.B. Yang and M.Donath, Dynamic model of a two-link robot manipulator with both structural and joint flexibility, in: Proceedings of the ASME 1988 Winter Annual Meeting, Chicago, 1988, pp.37-44.

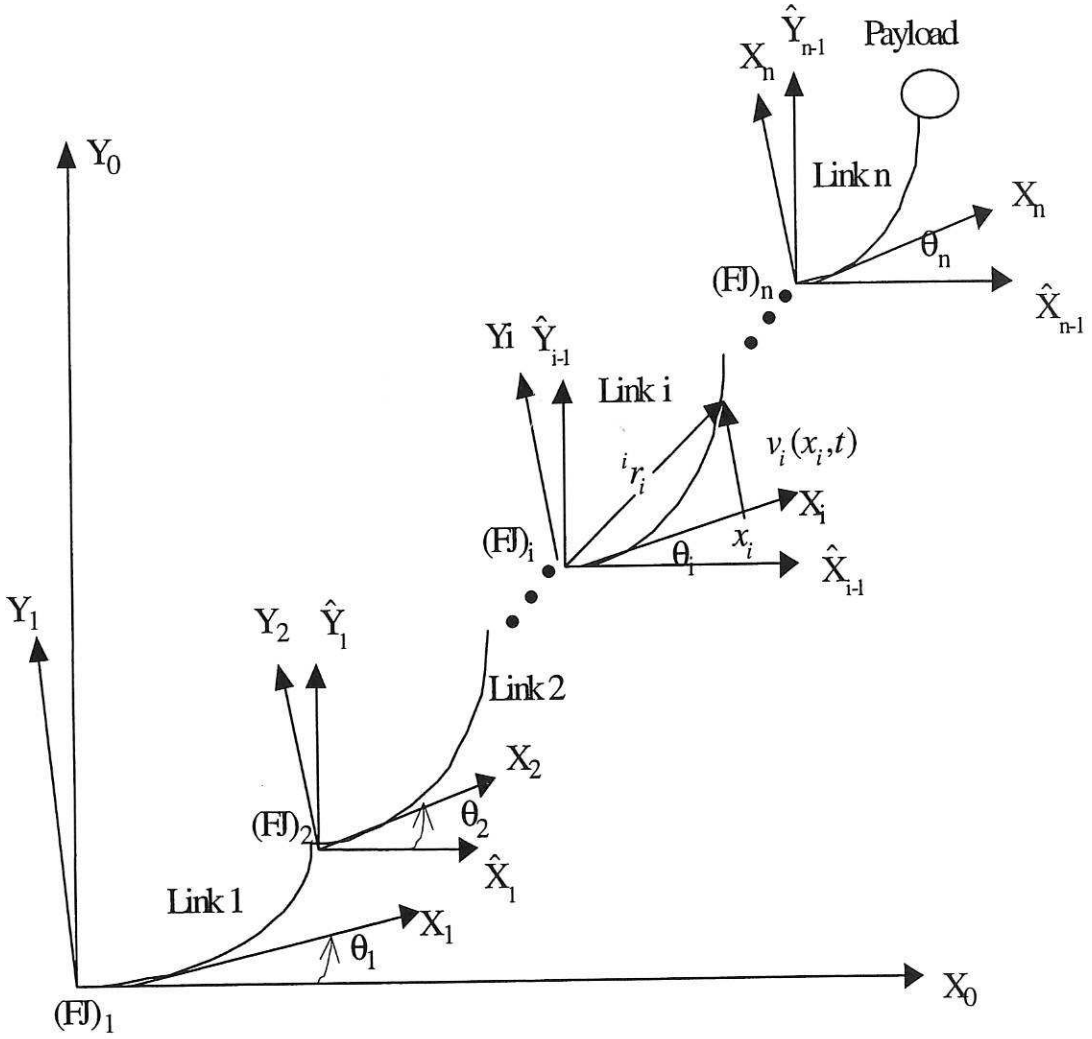

Fig.1 Multiple flexible links and flexible joints manipulator

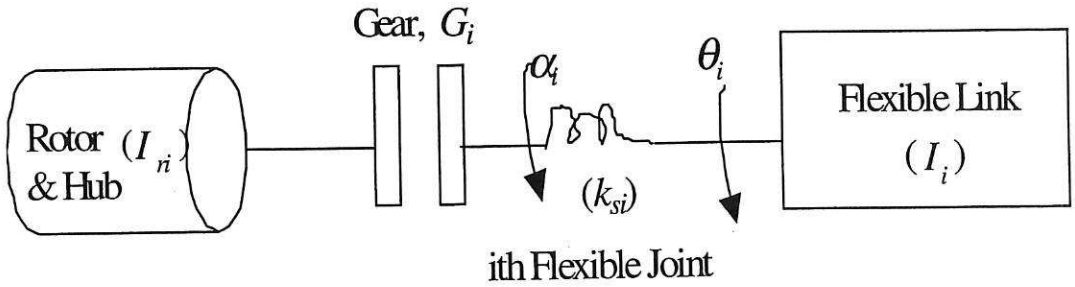

Fig.2 Schematic of flexible link and flexible joint assembly

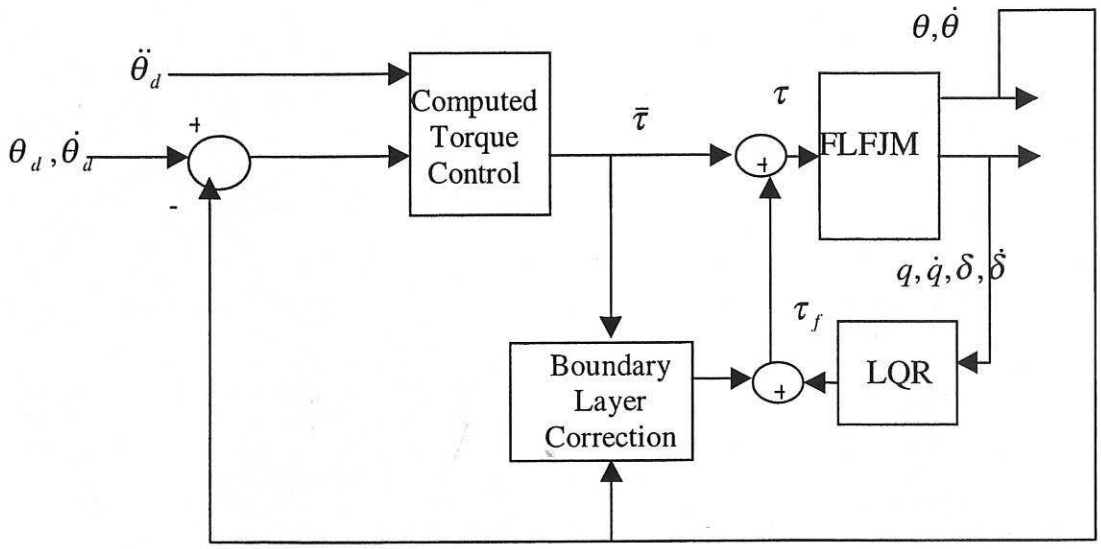

Fig.3 Composite control scheme

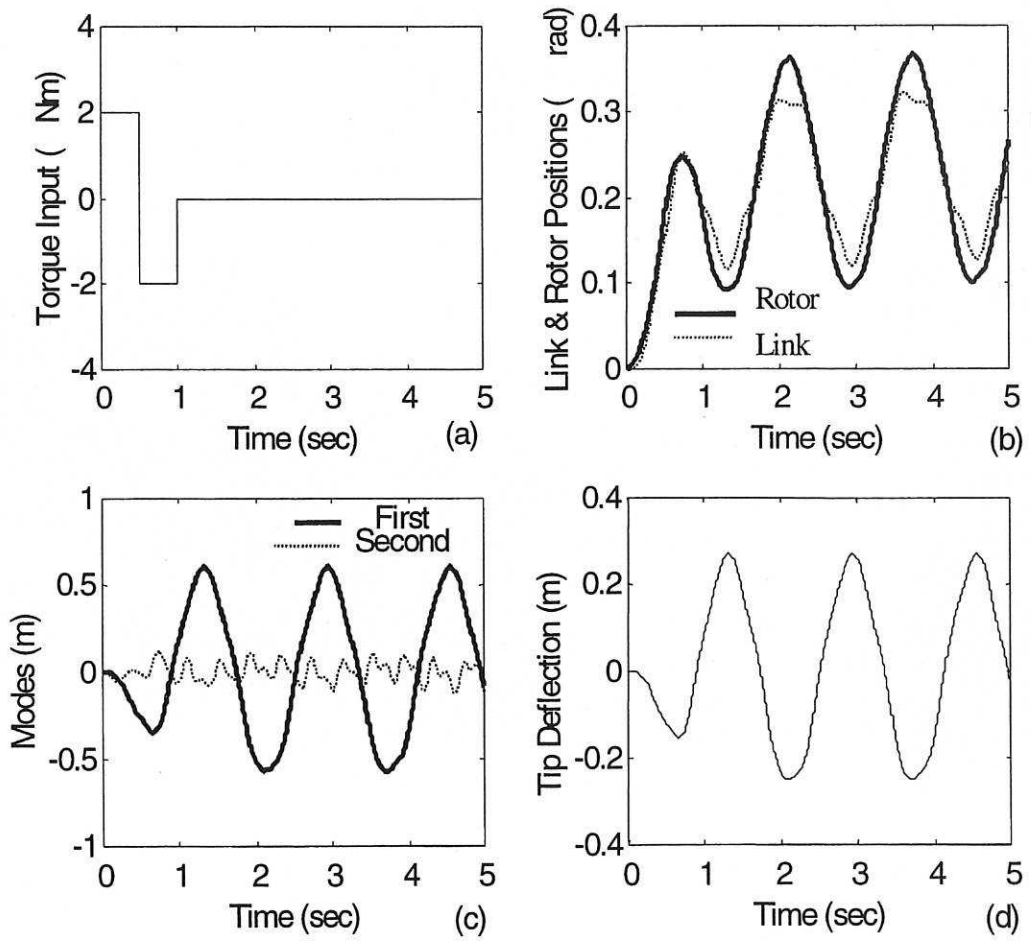

Fig.4 Model II responses to bang-bang torque input

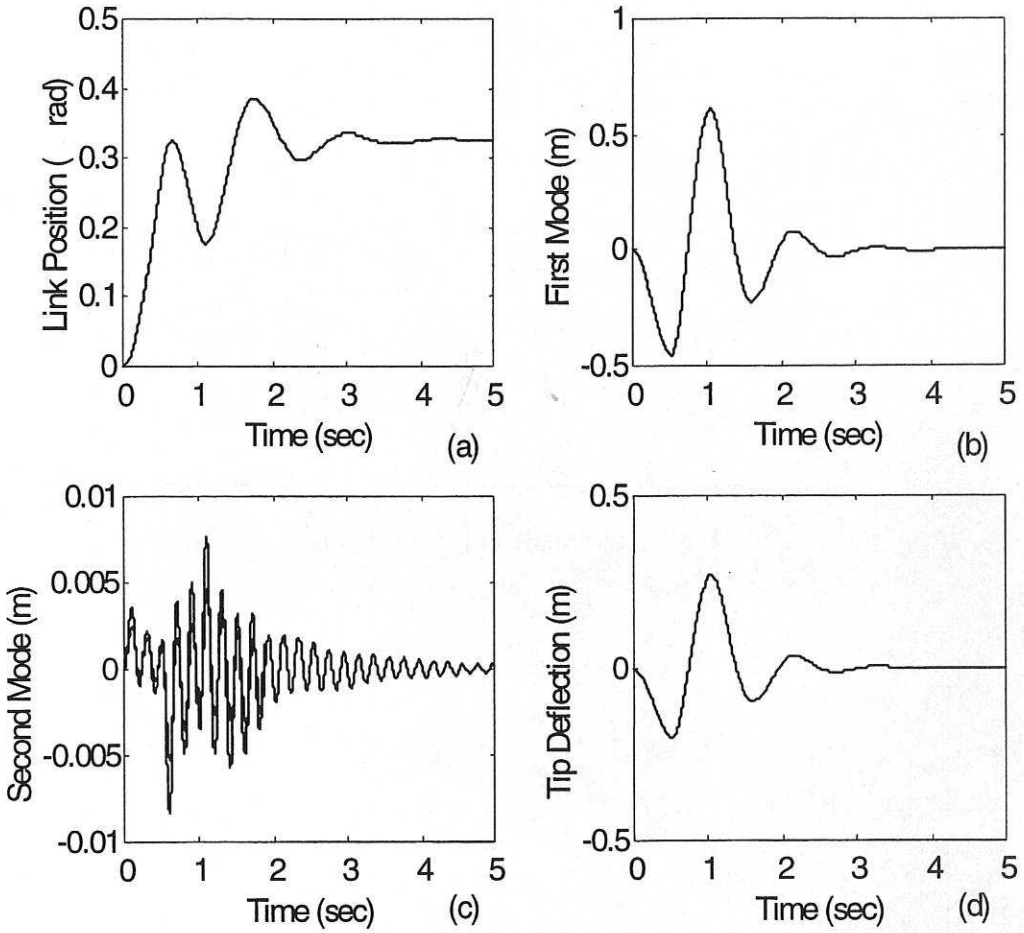

Fig. 5 Model I responses to bang bang input torque

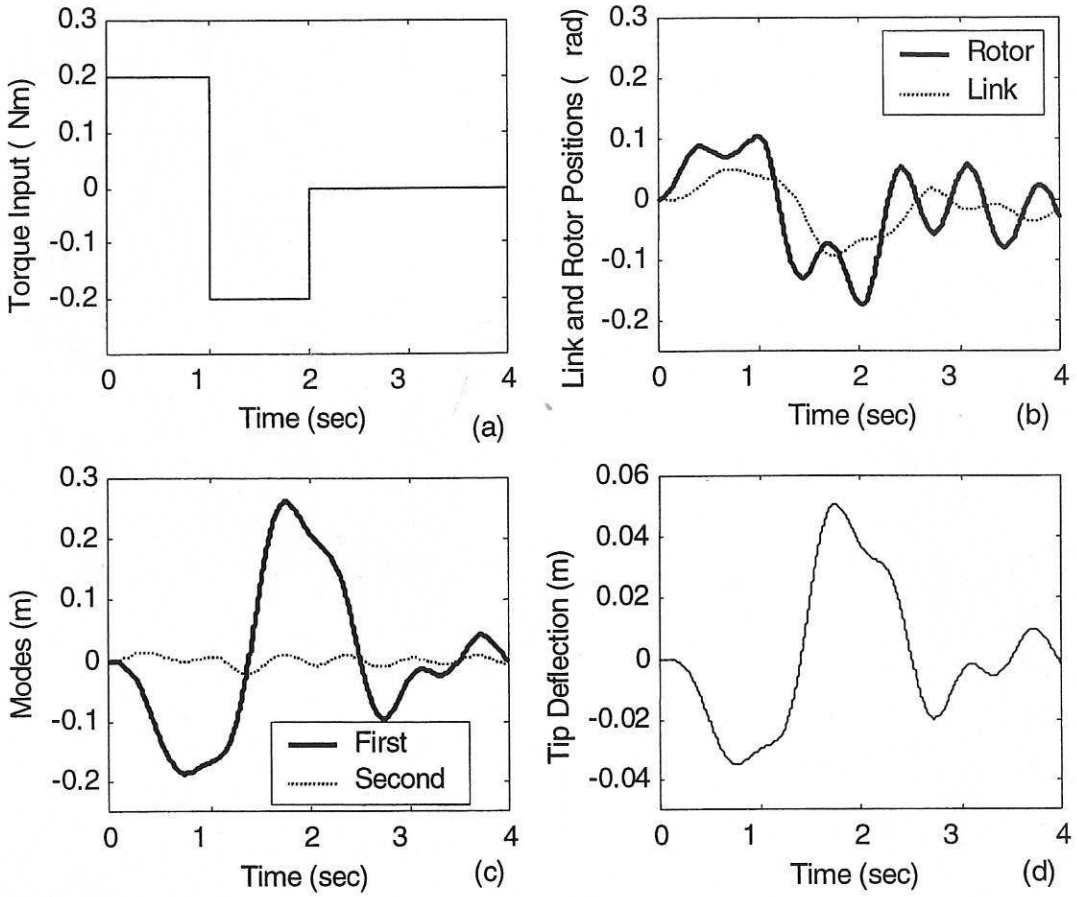

Fig.6 Responses of model IV to bang-bang torques (link 1 and rotor1)

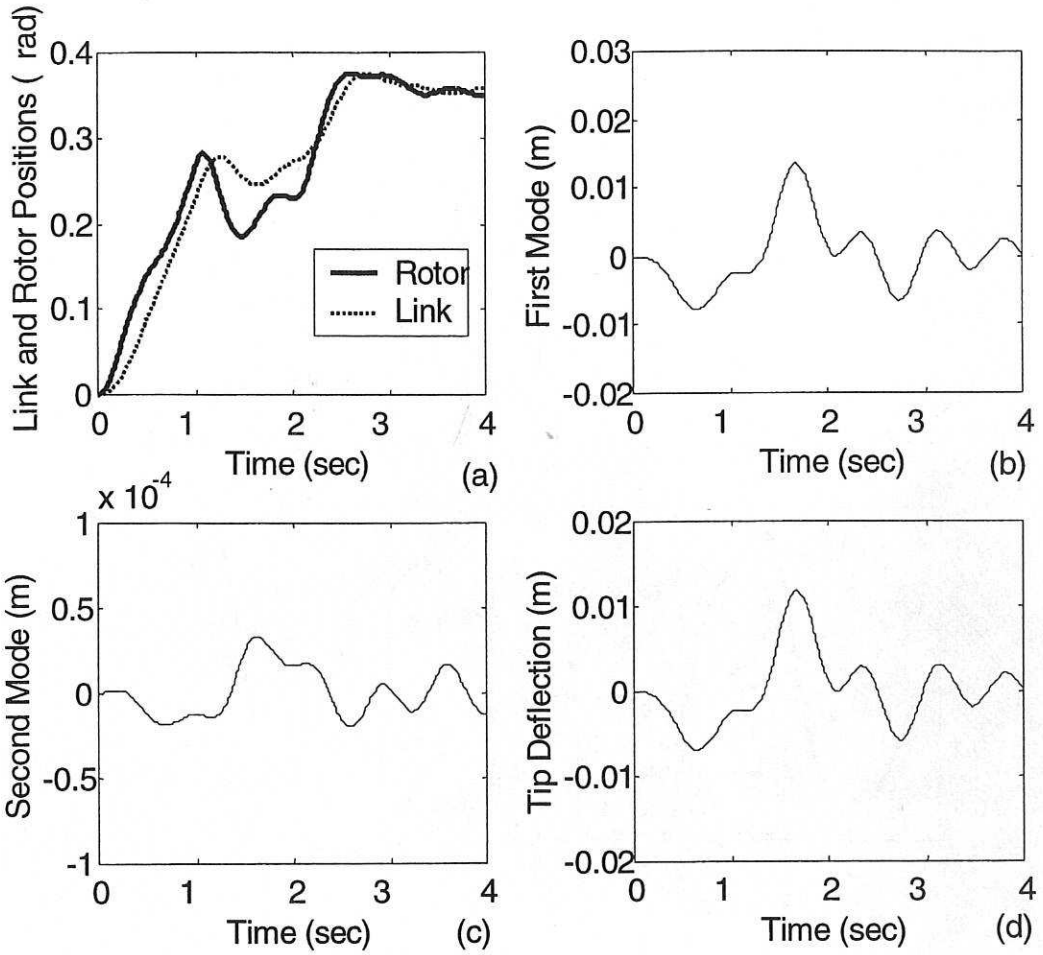

Fig. 7 Responses of model IV to bang-bang torque (link2 and rotor2)

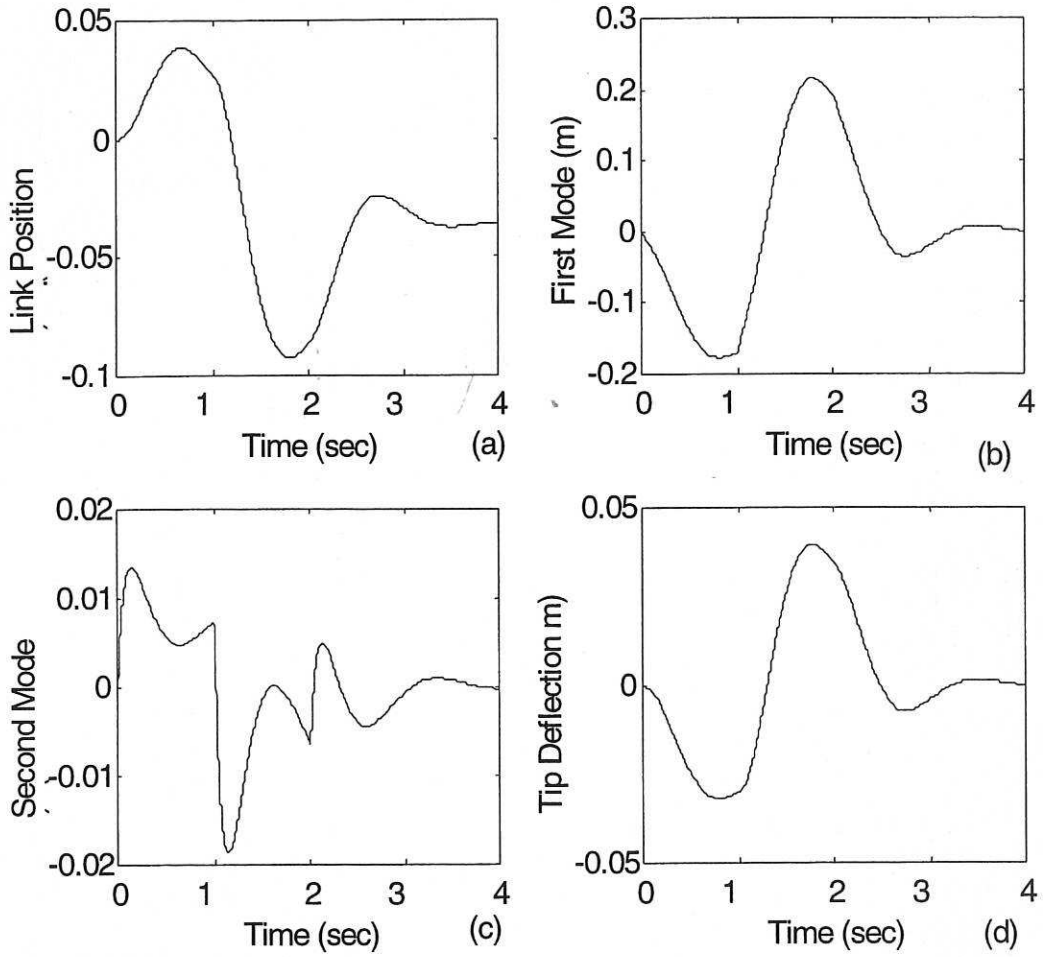

Fig.8 Responses of model III to bang-bang torque inputs (link 1)

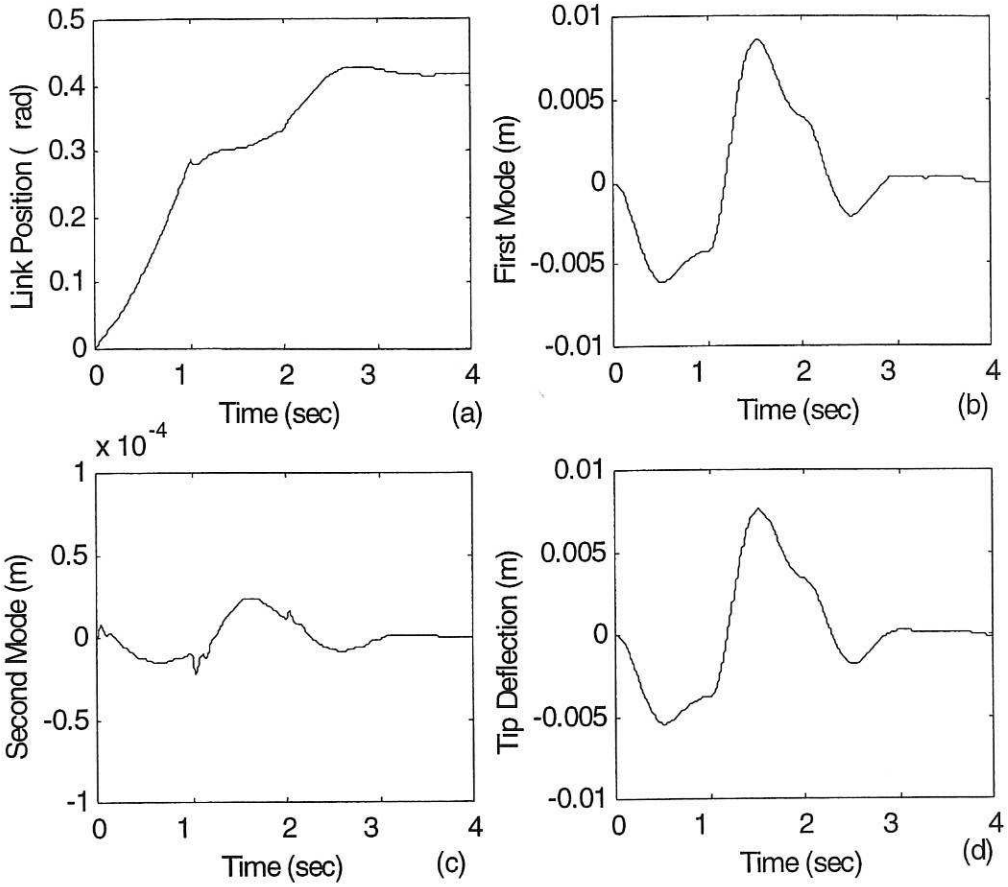

Fig.9 Responses of model III to bang-bang torque inputs (link 2)

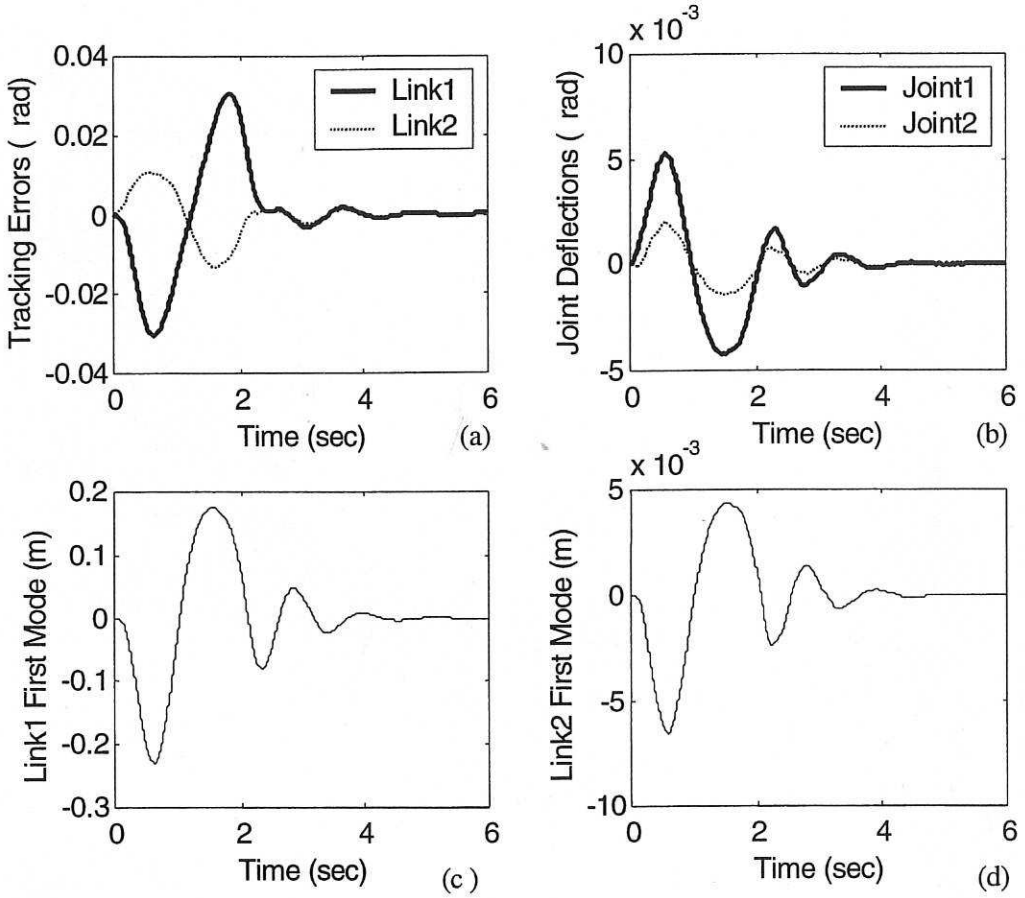

Fig.10. Controller performance((a) tracking desired trajectories, (b)damping joint deflections, (c) link1 first modal vibration and, (d) link2 second mode trajectory)

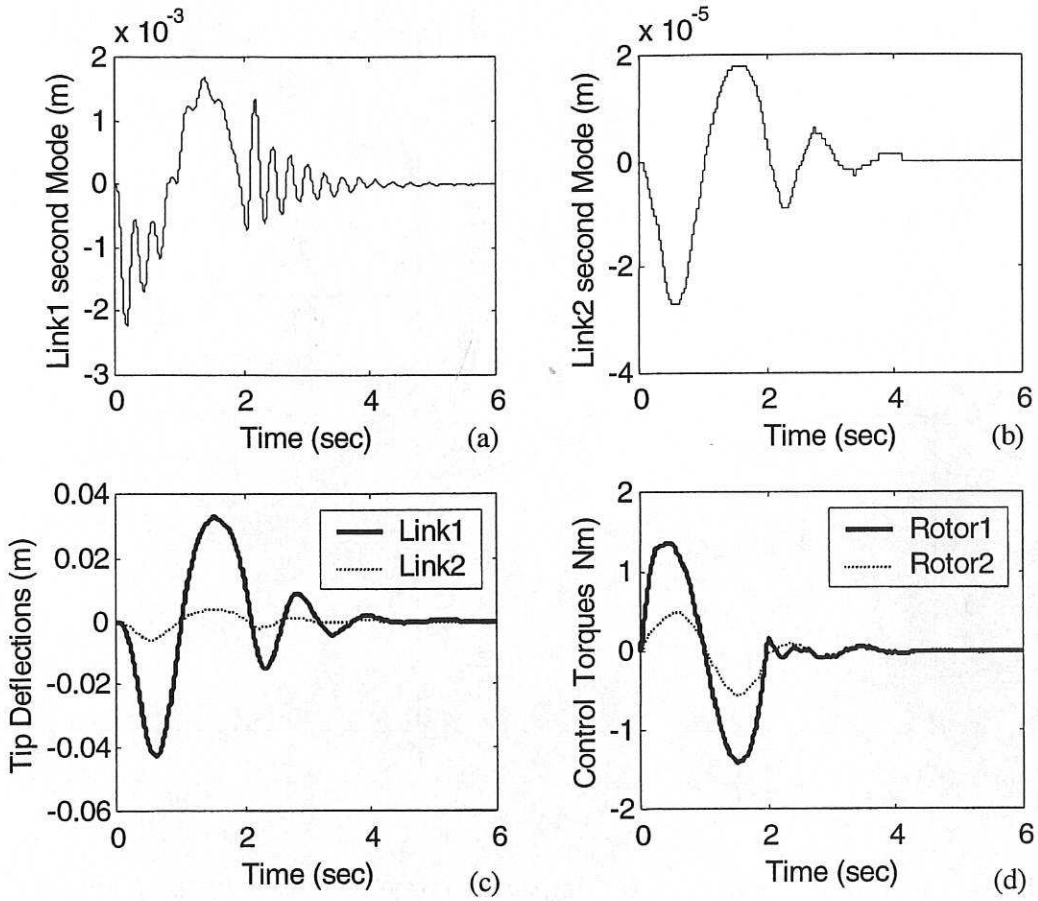

Fig.11. Controller performance ((a) link1 second mode trajectory, (b) link2 second mode trajectory, (c) tip deflections control and, (d) control torque signals generated)

Table 1 Parameters of the models I and II

Parameter	Value
Link length(l)	2.0 m
Mass Density(ρ)	0.1569 Kgm^{-2}
Flexural Rigidity(EI)	31.75 Nm^{-2}
Rotor and hub Inertia(I_r)	0.01865 Kgm^2
Payload (M_P)	0.2 Kg
Damping constants(d_1, d_2)	0.2

Table 2 Parameters of the models III and IV

Parameter	Value
Mass density (ρ)	0.2 Kgm^{-1}
Flexural rigidity(EI)	1.0 Nm^2
Length (l)	0.5m
Rotor and hub Inertia(I_r)	0.02 Kgm^2
Payload mass (M_p)	0.1 Kg
Payload Inertia (I_p)	0.005 Kgm^2
Damping constants (d_{11}, d_{12}, d_{13}, d_{14})	0.015, 0.02, 0.015, 0.02

UNIV OF SHEFFIELD LIBRARY ST. GEORGES